

Atom-superposition and electron-delocalization tight-binding band theory

K. Nath and Alfred B. Anderson

Department of Chemistry, Case Western Reserve University, Cleveland, Ohio 44106

(Received 23 December 1988; revised manuscript received 11 December 1989)

The atom-superposition and electron-delocalization band theory introduced recently for covalent solids is tested on metallic and ionic solids. Full details of the method are given. Its merits and demerits are discussed. Atomization energies, bulk moduli, energy gaps, and electronic densities of states are compared with experimental and other theoretical results where available.

INTRODUCTION

The semiempirical atom-superposition and electron-delocalization molecular-orbital (ASED-MO) theory^{1,2} is used to calculate structures, vibrational force constants, stabilities, reaction energies and pathways, and electronic properties of molecules and clusters of atoms. For determining solid-state properties cluster models have been used, for example, to calculate lattice constants and force constants for covalently bonded solids,³ and for predicting defect structures in cation-deficient ionic-transition-metal monoxides.⁴ Interfacial adhesion of metal and ceramic surfaces has also been modeled⁵⁻⁷ as have many chemisorption phenomena.⁸

A band version of this ASED method has recently been developed and applied in predicting structural and electronic properties of C, Si, and some simple polytypes of SiC.⁹ The comparison of ASED band-structure results with results of other semiempirical methods and with *ab initio* methods based on the Hohenberg-Kohn-Sham density-functional approach was very favorable for these covalent materials. The band version of the ASED approach is preferable, in principle, to the ASED-MO cluster-model approach for calculating properties of solids and surfaces. The CaF₂/Si(111) interface has been characterized recently¹⁰ using ASED band and cluster MO models. Interestingly, the slab band calculations confirmed the applicability of the use of small-cluster models for studying interfacial binding.

This paper presents the details behind the earlier communication⁹ and tests the method on oxides (BeO, MgO, and FeO), on an ionic material (CaF₂), on a ferromagnetic metal (Fe), and on relatively-free-electron metals (Al, Ni, and Cu).

METHOD

The atom-superposition and electron-delocalization molecular-orbital theory is based on a charge-density-partitioning method. The electronic charge density of a molecule or a solid can be partitioned in any number of ways. In the present theory partitioning is into perfectly-following (on the nuclei) spherical atomic components and the non-perfectly-following remainder. The theory is most easily demonstrated for a diatomic *ab*, from which the generalization to triatomics or to bigger

clusters or to solids is straightforward.

The molecular charge density for the diatomic molecule *ab* is given by

$$\rho(\mathbf{r}, \mathbf{R}_a, \mathbf{R}_b) = \rho_a(\mathbf{r} - \mathbf{R}_a) + \rho_b(\mathbf{r} - \mathbf{R}_b) + \rho_{npf}(\mathbf{r}, \mathbf{R}_a, \mathbf{R}_b), \quad (1)$$

where \mathbf{r} and \mathbf{R} are electron and nuclear coordinates with respect to an arbitrary origin. When assigning the origin of coordinates to nucleus *a*, the electrostatic force on nucleus *b* is given in terms of two components as follows:

$$\mathbf{F}(\mathbf{R}_b) = \mathbf{F}(\mathbf{R}_b, \rho_a, Z_a) + \mathbf{F}(\mathbf{R}_b, \rho_{npf}). \quad (2)$$

The integration of Eq. (2) yields the energy of interaction:

$$E(\mathbf{R}_b) = E_R(\mathbf{R}_b) + E_{npf}(\mathbf{R}_b), \quad (3)$$

where

$$E_R(\mathbf{R}_b) = Z_b \left[\frac{Z_a}{R_b} - \int \frac{\rho_a(\mathbf{r})}{|\mathbf{r} - \mathbf{R}_b|} d\mathbf{r} \right] \quad (4)$$

is the electrostatic energy of nucleus *b* in the presence of fixed atom *a*, and Z_a and Z_b are the respective nuclear charges of atoms *a* and *b*. This part of the energy is always positive (repulsive), hence the subscript *R*. The second term in Eq. (3) accounts for the energy due to the electronic charge rearrangement attendant to bond formation and is given by

$$E_{npf}(\mathbf{R}_b) = -Z_b \int_{-\infty}^{|\mathbf{R}_b|} \int \rho_{npf}(\mathbf{r}, \mathbf{R}_b') \frac{d}{d\mathbf{R}_b'} \frac{1}{|\mathbf{R}_b' - \mathbf{r}|} d\mathbf{r} d\mathbf{R}_b'. \quad (5)$$

For infinite separation of the atoms, $E(\mathbf{R}_b)$ is taken as the isolated-atom energy. The size of E_R and E_{npf} , of course, depends on which of the two nuclei is fixed as the reference point; the total energy is, however, invariant. E_R is readily calculated from available atomic-orbital wave functions. E_{npf} requires knowledge of ρ_{npf} , which is not available. It has been shown¹ that an extended Hückel-like delocalization energy is generally a good approximation of E_{npf} . In this approach the diagonal elements H_{ii}^{aa} are set equal to the negative of the measured ionization potential (V_{IP}) of valence level *i* on atom *a*. The off-diagonal elements on the same atom are zero by

orthogonality, i.e.,

$$H_{ij}^{aa} = -\delta_{ij} (V_{IP})_i^a. \quad (6)$$

The remaining off-diagonal elements are

$$H_{ij}^{ab} = 1.125(H_{ii}^{aa} + H_{jj}^{bb})S_{ij}^{ab} \exp(-0.13R_{ab}), \quad (7)$$

with

$$S_{ij}^{ab} = \langle \psi_i^a | \psi_j^b \rangle \quad (8)$$

being the overlap integral between the i th atomic orbital on atom a and the j th orbital on b , the latter being a distance R_{ab} (Å) away. In summary, one can write the Hamiltonian, from which E_{npf} is obtained by diagonalization, as

$$\hat{H} = \sum_{i,a} H_{ii}^{aa} |\psi_i^a\rangle \langle \psi_i^a| + \sum_{a,b,i,j} H_{ij}^{ab} |\psi_i^a\rangle \langle \psi_j^b|. \quad (9)$$

When this approximation to E_{npf} is used, results are generally more accurate if the two-body energy, E_R , is calculated using the charge density of the more electronegative atom for ρ_a in Eq. (4). Slater-orbital basis functions have been employed in the present as well as in past work. The semiempirical ASED-MO theory is a way of generating molecular properties from atomic data. Small changes in the parameters may be required and rules for this have been developed. This is discussed later.

The ASED valence-band calculations for bulk solids use the Hamiltonian given by Eqs. (6)–(9) in the usual tight-binding way.¹¹ $\{\psi_1, \psi_2, \dots, \psi_n\}$ is the set of Slater-type orbitals (STO's) centered on nuclei of the primitive unit cell. A set of Bloch functions $\{\phi_1(\mathbf{k}), \phi_2(\mathbf{k}), \dots, \phi_n(\mathbf{k})\}$ are constructed from them:

$$\phi_\mu(\mathbf{r}, \mathbf{k}) = \frac{1}{N} \sum_{p=1}^N e^{i\mathbf{k}\cdot\mathbf{R}_p} \psi_\mu(\mathbf{r} - \mathbf{R}_p), \quad (10)$$

where N is the number of primitive unit cells in the system. The band orbitals $\chi_j(\mathbf{r}, \mathbf{k})$ ($j = 1, 2, \dots, n$) are given by a linear combination of these Bloch functions:

$$\chi_j(\mathbf{r}, \mathbf{k}) = \sum_{\mu=1}^n C_{\mu j} \phi_\mu(\mathbf{r}, \mathbf{k}). \quad (11)$$

The C 's are generated during the diagonalization of the secular determinant,

$$|H_{\mu\nu}(\mathbf{k}) - S_{\mu\nu}(\mathbf{k})\epsilon(\mathbf{k})| = 0, \quad (12)$$

which also gives the band energies of $\epsilon_\eta(\mathbf{k})$, η being the band index ($\eta = 1, 2, \dots, n$). The $(\mu\nu)$ th matrix element of the Bloch Hamiltonian is given by

$$\begin{aligned} H_{\mu\nu}(\mathbf{k}) &= \langle \phi_\mu(\mathbf{r}, \mathbf{k}) | \hat{H} | \phi_\nu(\mathbf{r}, \mathbf{k}) \rangle \\ &= \frac{1}{N} \sum_{p,q=1}^N e^{i\mathbf{k}\cdot(\mathbf{R}_q - \mathbf{R}_p)} \langle \psi_\mu(\mathbf{r} - \mathbf{R}_p) | \hat{H} | \psi_\nu(\mathbf{r} - \mathbf{R}_q) \rangle. \end{aligned} \quad (13)$$

The matrix elements of the operator \hat{H} on the right-hand side are the same $H_{\mu\nu}^{pq}$ given by Eq. (7). The overlap integral is

$$\begin{aligned} S_{\mu\nu}(\mathbf{k}) &= \langle \phi_\mu(\mathbf{r}, \mathbf{k}) | \phi_\nu(\mathbf{r}, \mathbf{k}) \rangle \\ &= \frac{1}{N} \sum_{p,q=1}^N e^{i\mathbf{k}\cdot(\mathbf{R}_q - \mathbf{R}_p)} \langle \psi_\mu(\mathbf{r} - \mathbf{R}_p) | \psi_\nu(\mathbf{r} - \mathbf{R}_q) \rangle \\ &= \frac{1}{N} \sum_{p,q=1}^N e^{i\mathbf{k}\cdot(\mathbf{R}_q - \mathbf{R}_p)} S_{\mu\nu}^{pq}. \end{aligned} \quad (14)$$

Again, $S_{\mu\nu}^{pq}$ is the same as given by Eq. (8).

The energy, E_B^P , per primitive unit cell is found by integrating:

$$E_B^P = \frac{\int \sum_i n_i \epsilon_i(\mathbf{k}) d\mathbf{k}}{\int d\mathbf{k}}. \quad (15)$$

The integrations are over the first Brillouin zone, i spans the band index, and n_i are the orbital occupation number (0, 1, or 2). In terms of density of states, $g(\epsilon)$ (which is proportional to the inverse of the gradient of energy with respect to the wave vector), Eq. (15) can be written as

$$E_B^P = \frac{1}{N} \sum_i n_i \int \epsilon_i g(\epsilon_i) d\epsilon_i, \quad (16)$$

keeping in mind that the electronic states are evenly distributed in \mathbf{k} space. The integration range is from $-\infty$ to the Fermi energy, E_F . For a solid, the atomization energy per primitive unit cell, E^P , can now be given as

$$E^P = E_R^P + E_B^P - \sum_a \sum_i n_i \epsilon_{ai}^{AO}, \quad (17)$$

where E_R^P is the total two-body repulsion energy, E_R , from summing the pairwise interaction within the primitive cell and half of the pairwise interactions between the atoms of the primitive cell and those of the neighboring ones. ϵ_{ai}^{AO} is the atomic valence-state ionization energy of the i th level on atom a within a primitive cell. E_B^P as defined by Eq. (15) or (16) is calculated either by integration in half of the first Brillouin zone or with help of the special \mathbf{k} points as prescribed by Chadi and Cohen¹² and by Cunningham.¹³ Bulk moduli of the materials can easily be calculated using the relation

$$B_0 = -V_0 \frac{\partial P}{\partial V} = V_0 \frac{\partial^2 E^P}{\partial V^2}, \quad (18)$$

where V_0 is the equilibrium volume of the primitive unit cell. For some simple crystal structures, working formulas to obtain bulk moduli are given in Table I.

For all the properties calculated, the overlap integrals in the Bloch Hamiltonian were evaluated for centers up to 10 Å apart, except for BeO and MgO systems, for which 15 Å was used because Be^+ and Mg^+ valence orbitals are relatively large. Except for the hexagonal systems, special \mathbf{k} -point sets were employed. For three-dimensional (3D) hexagonal systems the integrations were done in a quarter of the first Brillouin zone and for 2D systems in half of it.

COMPARISON OF ACCURACY USING SPECIAL \mathbf{k} POINTS VERSUS THE FULL BRILLOUIN ZONE

Energy, charge density, dipole matrix elements, etc. are periodic functions of wave vector \mathbf{k} in the Brillouin zone

TABLE I. Working formulas to calculate bulk moduli of some simple crystal structures. E^p is the total energy per primitive unit cell, and x is the nearest-neighbor distance between two atoms in the crystal. The values obtained are in eV \AA^{-3} , and can be expressed in GPa upon multiplication by 160.2.

Crystal structure	Working formula
Zinc-blende structure	$(16\sqrt{3})^{-1} \frac{1}{x} \frac{\partial^2 E^p}{\partial x^2}$
Wurtzite structure	$(32\sqrt{3})^{-1} \frac{1}{x} \frac{\partial^2 E^p}{\partial x^2}$
Sodium chloride structure	$(18)^{-1} \frac{1}{x} \frac{\partial^2 E^p}{\partial x^2}$
bcc	$(4\sqrt{3})^{-1} \frac{1}{x} \frac{\partial^2 E^p}{\partial x^2}$
fcc	$\sqrt{2}/9 \frac{1}{x} \frac{\partial^2 E^p}{\partial x^2}$
hcp	$2 \left[9\sqrt{3} \frac{c}{a} \right]^{-1} \frac{1}{x} \frac{\partial^2 E^p}{\partial x^2}$

(BZ). For example, to get the energy per primitive cell involves averaging $\epsilon(\mathbf{k})$ over the BZ. Besides translational invariance, these functions can be invariant under certain point-group or space-group operations or both, depending on the nature of the Bravais lattice. Using these properties, the BZ can be reduced to smaller zones. An irreducible (smallest) wedge of the BZ contains most of the information on the full BZ. Using this fact, Chadi and Cohen¹² have determined certain special- \mathbf{k} -point sets for crystals with cubic and hexagonal 3D Bravais lattices. Using their scheme, Cunningham¹³ has obtained some special- \mathbf{k} -point sets in the two-dimensional BZ for oblique, centered-rectangular, primitive rectangular, square, and hexagonal lattices. Averaging over this 2D BZ is needed for calculations such as the surface mean-square displacement, the surface Debye-Waller factor, and, as demonstrated recently, for adhesion and interface studies.¹⁰ Averaging of any such property can be done by calculating its local values at these special \mathbf{k} points and summing them with proper weighting factors.

The accuracy of results based on these special \mathbf{k} points has been checked for various lattices. It is found that the 10 special \mathbf{k} points for a fcc-lattice material gives bond lengths precise to 0.01 \AA , energy to 0.01 eV, and bulk

modulus (or second derivative of the energy with respect to nearest-neighbor distances) to within 0.5%. The same is not true for the hexagonal (2D or 3D) systems studied. This is demonstrated here for cubic and hexagonal structures of Si. The results are presented in Table II.

For cubic Si the atomization energy based on the 10-special- \mathbf{k} -point set is 3.744 eV, essentially the same as the converged result of integration in half [since $E(\mathbf{k})=E(-\mathbf{k})$] of the first BZ. The bond length and bulk modulus also remain unchanged. For hexagonal Si the 12-special- \mathbf{k} -point set gives an atomization energy which is 7% higher than the converged integrated result. The bond length is 0.01 \AA shorter and the bulk modulus is overestimated by 3%.

For Fe in the bcc structure, the eight-special- \mathbf{k} -point set of Chadi and Cohen gives, to three significant figures, the same atomization energy and bulk modulus as the converged values. However, this special- \mathbf{k} -point set also gives an equilibrium bond length 0.01 \AA larger than the converged result, which is a difference in the third significant figure.

RULES FOR THE PARAMETER SELECTION IN GENERAL

The gas-phase free-atom Slater exponents, ζ 's, for non-transition elements are taken from Clementi and Raimondi.¹⁴ Where exponents for p orbitals are not available, they are usually assumed to be 0.3 a.u. smaller than the corresponding s orbitals. For the first-row transition-metal atoms, the exponents are from Richardson *et al.*¹⁵ with $4s$ exponents taken 0.3 a.u. larger than the reported ones and $4p$ ones taken 0.3 a.u. smaller than the $4s$ exponents used, the usual practice for ASED-MO calculations. For the d orbitals, double- ζ functions from Ref. 15 are used. The change, if required, to get the proper bond length, is made only to the s , p , and the smaller of the two d exponents. The valence-state ionization potentials (IP's) are taken from Lotz¹⁶ and from Moore.¹⁷ Clementi and Roetti¹⁸ have also reported the multi- ζ exponents for cations, anions, and neutral atoms. Since the ASED-MO and band programs use single- ζ s and p functions, a simple averaging is done by weighting the multi- ζ exponents with the corresponding coefficients.

In the process of doing band calculations, the dimer or diatom properties are studied first using the ASED-MO method. These include the bond lengths, dissociation energies, charge transfers (for binary systems, based on

TABLE II. Comparison of results for cubic and hexagonal Si, and for bcc Fe, based on special \mathbf{k} points of Chadi and Cohen (Ref. 12) and on converged numerical integration in the first BZ. R_c (\AA) denotes bond length, E_A (eV) atomization energy, and B_0 (GPa) the bulk modulus.

	Cubic Si results		Hexagonal Si results		bcc Fe results	
	10 special \mathbf{k} points	Converged values ^a	12 special \mathbf{k} points	Converged values ^a	8 special \mathbf{k} points	Converged values ^a
R_c	2.36	2.36 ^a	2.35	2.36 ^a	2.48	2.47
E_A	3.744	3.743	3.987	3.737	3.503	3.504
B_0	112.5	112.7	116.0	113.1	202.0	201.9

^aAround 1000 points in the BZ give the converged values.

Mulliken population analysis), and occasionally the vibrational force constants. These properties are compared with the experimental results, where available. The calculated charge transfer is compared with an ionicity versus electronegativity difference relationship. Frequently, for ionic and sometimes also for covalent materials, a change from the experimental V_{IP} input parameterization is required to get the proper charge transfer. This is usually done by increasing the smaller V_{IP} and decreasing the larger V_{IP} by the same amount in steps of 0.1 eV. The exponents are scaled at the same time to get the correct experimental bulk bond length.

For oxides such as BeO and MgO, the cation exponents are taken from the literature¹⁸ and the literature oxygen exponents¹⁴ are scaled to get the correct nearest-neighbor bulk distances. All the parameters used are given in Table III. The specific procedures for individual solids are given with each case study below.

RESULTS

First, we discuss equilibrium bond lengths, atomization energies, bulk moduli, band gaps, and charge transfers (Table IV). The results for diamond, graphite, silicon, and α - and β -SiC were reported earlier,⁹ where comparisons were made with unadjusted parameters and also with empirical and theoretical calculations of others. The results for Fe, FeO, MgO, BeO, CaF₂, Al, Cu, and Ni, presented in Table IV for the first time, are similarly compared with the literature here. Calculated electronic densities of states are given in Fig. 1 for some of these systems, with comparisons to available experimental results; this is discussed at the end of the paper.

A scaling factor of 1.13 for the s and p exponents of carbon gives bond lengths of 1.53 and 1.42 Å, respectively, for diamond and graphite compared to the observed values of 1.54 and 1.42 Å. In agreement with experiment, graphite is calculated to be more stable than diamond. The calculated atomization energy, E_A , for diamond is 10% larger than the experimental value. The bulk modulus, B_0 , and the band gap are 22% larger and 43% smaller, respectively, compared to the experimental results. For graphite the atomization energy is 12% larger than the observed value and the energy-band gap is correctly predicted to be zero. Not mentioned in Ref. 9 is the finding that the hexagonal structure of diamond is energetically 0.33% less stable than the cubic structure, and its bond length is 0.12% larger as well.

For Si a scaling factor of 1.04 gives a bond length of 2.36 Å, which is within 0.01 Å of the observed value. The atomization energy is 20% smaller and the bulk modulus is 14% larger than the experimental values. The energy gap is 1.74 eV compared to the observed value of ~ 1.17 eV. The cubic structure of Si is more stable than the hexagonal structure, in agreement with experiment (Table II).

For diatomic SiC the IP's of Si are increased by 1.3 eV and those of C are decreased by this amount to get a charge transfer close to the expected ionicity based on the electronegativity difference. To approach the observed

bulk bond length of 1.89 Å, C bulk exponents and Si bulk exponents were, as discussed above, multiplied by and divided by 0.9, respectively. This can be thought of as making the C atom bigger in the crystal and the Si atom smaller. These parameters give the bond length to within 0.01 Å. The cubic β -SiC structure is calculated to be more stable than the wurtzite α -SiC structure, which agrees with experiment. The atomization energies for both structures are underestimated by 6%, whereas the bulk moduli are overestimated by 17%. The energy gap obtained is 55% larger for the cubic structure, whereas it is only 8% larger for the hexagonal ($2H$) structure. There is an electron charge transfer of -0.47 from Si to C, and only -0.2 for diatomic SiC.

For bulk bcc Fe the spin polarization is 2.12.¹⁹ This can be thought of as 5.06 of the eight valence electrons in the primitive cell having spin up in the s - d -hybridized band and 2.94 having spin down. Keeping this in mind, the right-hand side of Eq. (16) is integrated (using Simpson's rule) up to some intermediate-energy value, lower than E_F (the Fermi energy), with double-electron occupation and then up to E_F with single-electron occupation. A scaling factor of 1.07 to the exponents (except for the contracted d one, which we do not usually change) gives a bulk bond length of 2.47 Å, within 0.01 Å of the experimentally observed value. For the purpose of calculating the two-body energy per primitive cell, E_R^p , the initial Fe-atom orbital occupation is taken as $4s^1 3d^7$. Compared to experiment, the predicted atomization energy and bulk modulus are 18% lower and 20% higher, respectively.

For diatomic FeO, an increase in the Fe IP of 1.9 eV and a decrease in the O IP of 0.4 eV gives a charge transfer close to the desired value. With these IP's and the scaled exponents, where Fe exponents are multiplied by 1.10 and O exponents are divided by 1.10 (or multiplied by 0.91), the bulk bond length obtained is the same as the experimental bond length, and the atomization energy is two-thirds of the experimental value. For bulk FeO the spin per primitive unit cell has been taken as 4 in order to occupy the d band up to the top. The Fe $4s$ band is destabilized and remains unoccupied. This gives an Fe $3d$ - $4s$ band gap of 6.3 eV, a bulk modulus of 123 GPa, and a charge transfer of $0.55 e^-$ from Fe to O.

For MgO the Mg exponents are taken as those for Mg^+ . Clementi and Roetti¹⁸ have given multi- ζ exponents for the Mg and Mg^+ $3s$ orbitals. The difference of the average of these two, 0.13 a.u., is added to the single- ζ exponent for the $3s$ orbital for Mg as given by Clementi and Raimondi¹⁴ to approximate for Mg^+ $3s$ single- ζ exponent. Since the $3p$ -orbital exponent is not available, it is taken as the same as $3s$. The diatomic MgO calculation suggests that an IP increase of 3.4 eV for Mg and the same amount of decrease for the O IP give a charge transfer close to the expected value. Having these parameters fixed, the O exponents are scaled to get the observed bulk bond length. A scaling factor of 0.89 gives the bond length to within 0.01 Å. The energy gap is overestimated by 17%. There is a charge transfer of $0.95 e^-$ from Mg to O and the calculated bulk modulus is 111 GPa. The atomization energy turns out

TABLE III. Parameters used in the calculations: principal quantum numbers n , ionization potentials [IP (eV)], Slater orbital exponents ζ (a.u.), and linear coefficients c , for double- ζ functions.

Atom	s			p			d			IP	
	n	ζ	IP	n	ζ	IP	n	c_1	c_2		ζ_2
C	2	1.8174	16.59	2	1.7717	11.26					
Si	3	1.6998	13.46	3	1.4855	8.151					
SiC	3	1.89	14.76	3	1.65	9.451					
C	2	1.64	15.29	2	1.59	9.96					
Fe	4	1.819	7.87	4	1.498	5.47	3	0.5555	0.6318	1.926	9.0
FeO	4	1.87	9.77	4	1.54	7.37	3	0.5518	0.6275	1.98	10.9
O	2	2.0437	26.98	2	2.0262	12.12					
MgO	3	1.23	11.046	3	1.23	6.624					
O	2	1.9988	25.08	2	1.9817	10.22					
BeO	2	1.1	10.622	2	1.1	7.897					
O	2	1.9538	27.18	2	1.9371	12.32					
CaF ₂	4	1.7	9.113	4	1.7	6.179					
F	2	1.9809	34.85	2	2.2041	14.42					
Al	3	1.4685	10.62	3	1.4501	6.986					
Cu	4	2.0165	7.73	4	1.6895	3.94	3	0.5698	0.5993	2.2890	10.4
Ni	4	1.998	7.64	4	1.665	4.45	3	0.5541	0.6135	2.22	10.0

to be only one-fourth of the experimental result. For highly ionic systems like this, the *ab initio* pseudopotential method within the local-density theory of Chang and Cohen²⁰ is more accurate.

For BeO the Be⁺ 2s exponent is obtained by adding 0.13 a.u. (assumed to be the same as in the case of Mg) to the Be 2s exponent. Again, the 2p exponent is taken to be the same as the 2s exponent. Shifts of 1.3 eV in the IP's

of Be and O towards each other give the proper charge transfer for the BeO diatom. A scaling factor of 0.87 to the O exponents gives a bulk bond length the same as the observed value of 1.65 Å. The structure is taken to be ideal wurtzite with a *c/a* ratio of $\sqrt{8/3}$. The atomization energy per chemical formula is only underestimated by 14% this time. The calculated bulk modulus is 210 GPa and the band gap is 9.3 eV, which is within the ex-

TABLE IV. Results for graphite, diamond, Si(cubic), cubic (3C) β -SiC, hexagonal (2H) α -SiC, Fe, FeO, MgO, BeO, CaF₂, Al, and Cu. R_e (Å), equilibrium bond length; E_A (eV), atomization energy (without zero-point corrections); B_0 (GPa), bulk modulus; ΔE (eV), band gap; q (*e*), atomic charge from Mulliken partitioning. The numbers in parentheses are experimental values.

Crystal	R_e^a	E_A^a	B_0^b	ΔE^c	q
C(gra)	1.42 (1.42)	8.23 (7.37)		0 (0)	
C(dia)	1.53 (1.5414)	8.05 (7.35)	539 (442)	3.07 (5.4)	
Si	2.36 (2.3516)	3.74 (4.68)	113 (98.8)	1.74 (1.17)	
β -SiC	1.88 (1.89)	12.0 (12.71)	261 (224)	3.71 (2.39)	Si, +0.47; C, -0.47
α -SiC	1.88 (1.89)	11.96 (12.69)	264 (225)	3.55 (3.3)	Si, +0.47; C, -0.47
Fe	2.47 (2.48)	3.50 (4.29)	202 (168.3)		
FeO	2.16 (2.16)	6.36 (9.68)	123	6.3	Fe, +0.55; O, -0.55
MgO	2.11 (2.105)	2.68 (10.27)	111 (155, 162)	9.1 (7.775)	Mg, +0.95; O, -0.95
BeO	1.65 (1.65)	10.45 (12.16)	210	9.3 (7.8-10.7)	Be, +0.57; O, -0.57
CaF ₂	2.36 (2.36)	11.17 (16.1)	23.4	9.55 (12.1)	Ca, +1.72; F, -0.86
Al	2.87 (2.86)	0.78 (3.36)	83 (72.2)		
Cu	2.56 (2.56)	0.932 (3.49)	76 (137)		
Ni	2.49 (2.49)	2.55 (4.43)	109 (186)		

^aExperimental values for 0 K from *CRC Handbook of Chemistry and Physics*, 67th ed., edited by R. W. Weast (Chemical Rubber Co., Boca Raton, FL, 1986).

^bReferences for experimental values: diamond and Si from F. Birch, in *Handbook of Physical Constants* [Geo. Soc. Am. Mem. **97**, 107 (1966)]; α -SiC and estimated for β -SiC from D. H. Yean and J. R., Riter, Jr., *J. Phys. Chem. Solids* **32**, 653 (1971), and references therein; Fe, Al, Cu, and Ni from C. Kittel, *Introduction to Solid State Physics*, edited by C. Kittel (Wiley, New York, 1986); MgO from M. J. L. Sangster, G. Peckham, and D. H. Saunderson, *J. Phys. C* **3**, 1026 (1970), and O. L. Anderson and P. Andreatch, Jr., *J. Am. Ceram. Soc.* **49**, 404 (1966).

^cReferences for experimental values: diamond and Si from C. Kittel (footnote b); α - and β -SiC from W. J. Choyke, *Mater. Res. Bull. (SiC Issue)* **4**, S141 (1969); MgO from R. C. Whited and W. C. Walker, *Phys. Rev. Lett.* **22**, 1428 (1969); BeO from A. P. Lukirskii and I. A. Byrtov, *Fiz. Tverd. Tela (Leningrad)* **6**, 43 (1964) [*Sov. Phys.—Solid State* **6**, 32 (1964)], D. M. Roessler and W. C. Walker, *J. Phys. Chem. Solids* **30**, 157 (1969), V. A. Fomichev, *Fiz. Tverd. Tela (Leningrad)* **13**, 907 (1971) [*Sov. Phys.—Solid State* **13**, 754 (1971)], and R. Gründler, K. Breuer, and W. Tews, *Phys. Status Solidi B* **86**, 329 (1978); CaF₂ from G. W. Rubloff, *Phys. Rev. B* **5**, 7526 (1987).

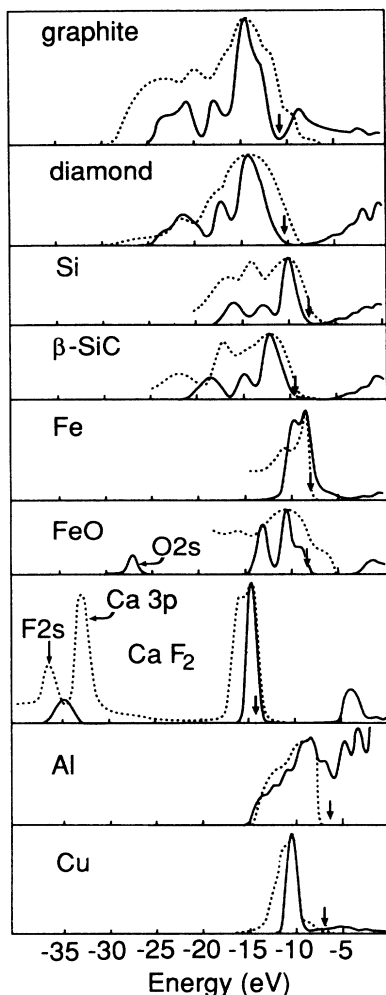


FIG. 1. Calculated (solid line) and experimental (dashed line) densities of states. Arrows show highest filled level in calculated curves. References to experimental curves are in the text.

perimental range 7.8–10.7 eV. The self-consistent calculation of Chang *et al.*²¹ has underestimated this value with a 7.0-eV result. There is a charge transfer of $0.57 e^-$ from Be to O.

For CaF_2 a set of Ca^{2+} exponents has to be defined. Clementi and Roetti¹⁸ give multi- ζ exponents for Ca and Ca^+ 4s orbitals. The difference of the average (with proper weight, taking the coefficients into account) of these two, 0.3 a.u., is added to the single- ζ exponent for Ca 4s as given by Clementi and Raimondi¹⁴ to get the single- ζ Ca^+ 4s exponent. Another 0.3 a.u. is added to this number to get the Ca^{2+} 4s exponent. The 4p exponent is assumed to be the same as the 4s exponent. The F^- 2s and 2p exponents are averaged multi- ζ values from Clementi and Roetti. There is a need for IP shifts of 3 eV to produce the proper charge transfer for the CaF diatom at the experimental distance of 1.97 Å. For bulk CaF_2 the 2s and 2p exponents of F^- are scaled by a factor 0.93 to get the experimental bond length of 2.36 Å. The atomization energy and band gap thus obtained are underestimated by 31% and 21%, respectively. There is a

charge transfer of $0.86 e^-$ to the F atoms; thus Ca becomes positive with a charge of 1.72. The calculated bulk modulus is 23.4 GPa.

For aluminum the literature parameters give a diatomic dissociation energy of only one-sixth of its experimental value. An increase in the p IP by 1 eV brings the p level closer to the resonance with the s level; thus the dissociation energy increases to about 80% of the experimental value when s and p exponents are decreased to get the experimental equilibrium internuclear distance. With these IP's and a scaling factor of 1.07 for the literature exponents, a bond length of 2.87 Å (the experimental value is 2.86 Å) is achieved for bulk aluminum. The bulk modulus thus obtained is overestimated by 15%, but the atomization energy is only one-quarter of the experimental value, whereas the *ab initio* calculation of Lam and Cohen²² has underestimated and overestimated the bulk modulus and the cohesive energy by only 1% and 7%, respectively.

For copper a scaling factor of 1.09 to the 4s, 4p, and 3d (uncontracted) exponents gives the experimental bond length, but only 55% for the bulk modulus and one-quarter for the atomization energy. For nickel a scaling factor of 1.11 to the exponents gives the experimental bond length. For bulk Ni the spin polarization is 0.55.¹⁹ Thus, on the average, 9.45 valence electrons per Ni atom are paired, and the rest, 0.55, is kept unpaired. This gives the atomization energy and the bulk modulus, which are 42% and 41% smaller than the respective experimental values. For the transition-metal series the two-body energy is calculated by assigning one of the valence electrons to the atomic s orbital and the remaining ones to the atomic d orbital, as was done for Fe.

Presented in Fig. 1 are calculated electronic densities of states (DOS's) for some of the systems studied above. Energy values have been approximated by Gaussian envelopes with a full width at half maximum (FWHM) of 1 eV. These are compared with experimental results. The height and position of the main peaks are aligned. No attempt has been made to match E_F . The arrows indicate the theoretical positions of the tops of occupied bands for the various crystals. For graphite the experimental curve is from x-ray photoemission spectroscopy (XPS) data²³ taken at 122 eV. The diamond result is compared with the soft-x-ray K -emission band.²⁴ The Si and β -SiC DOS's are compared with soft-x-ray K -emission and $L_{2,3}$ -emission bands superimposed with a 1:1 intensity ratio.²⁵ The Fe result is a spin-summed photoemission energy-distribution spectrum²⁶ (60-eV photons) taken at temperature $0.3T_C$, where T_C is the Curie temperature. For FeO a 30-eV photon photoemission energy-distribution curve²⁷ for Fe_{1-x}O is shown, where x is between 0.05 and 0.10. For CaF_2 a 150-eV photon photoemission spectrum²⁸ from a thick layer of CaF_2 on Si(111) is shown. In the theoretical calculation the Ca 3p core function has not been included. Had it been included in the calculations, it would have given a peak at ~ -31 eV which would have probably pushed down the F 2s peak and pushed up the F 2p peak by about 1 eV or so. For Al the ultraviolet photoemission spectroscopy spectrum is for 11.29-eV photons.²⁹ For Cu, XPS results are shown

for a vacuum-evaporated copper film with monochromatized Al $K\alpha$ radiation after background subtraction.³⁰ Looking at the DOS curves, it is apparent that the calculations underestimate the bandwidths while being able to produce general shapes of the experimental emission spectra. For CaF_2 and Cu the experimental shoulders are seen in the theory at smaller FWHM (~ 0.2 eV), but are not resolved in Fig. 1.

Besides comparing these band structures with the experimental results, they can also be compared with the theoretical results of others. For Fe the density of states of filled band orbitals is similar to that calculated by Callaway and Wang,³¹ but since they used different bands for spin-up and -down electrons, their density-of-states of empty orbitals is shifted to higher energy. The self-consistent-field calculation of Heaton and Lin³² produced a wider CaF_2 valence-band DOS than ours. Wider bandwidths will, in general, be obtained by the use of smaller valence-orbital exponents, but this will enlarge the bulk bond lengths. It is probable that using effective nuclear charges [Z_b in Eq. (4)] to decrease the two-body repulsion energy will allow the calculations to produce proper bandwidths and bond lengths at the same time. Our calculations and those of Heaton and Lin, however, underestimated the band gap of CaF_2 by the same amount. Our Al DOS is in very good agreement with experimental as well as theoretical³⁰ results. For Cu our DOS compares well with the augmented-plane-wave calculation of Burdick,³³ except that ours again has a smaller bandwidth (two d -band peaks merge together when fitted with 1.0-eV FWHM Gaussian functions).

CONCLUSIONS

The results clearly suggest that for ionic systems the theory underestimates atomization energies by about 25%, except for MgO, where the large IP shifts necessary for proper ionicity reduce the charge-transfer stabilization too much. In these systems ionic interactions of the Madelung form are expected to contribute to the atomization energies and the bulk moduli. Recently, an attempt has been made by Wang *et al.*³⁴ to include Madelung interactions in the extended Hückel Hamiltonian.

For the oxide systems, FeO, MgO, and BeO, and for CaF_2 , it seems that $\sim 10\%$ increases in cation exponents over their respective neutral-atom exponents and $\sim 10\%$ decreases in anion exponents over their respective neutral-atom exponents do a good job of reproducing many of the physical properties. The criterion of shifting

the IP parameter to yield atomic Mulliken charges in agreement with the ionicity calculated from the electronegativity difference gives nearly optimal results for the atomization energies and band gaps for all the materials except MgO.

The underestimate of cohesive energies for the s - p -valence-band metals Al and Cu and for the substantially s - p -band metal Ni reflects the general belief that plane waves constitute a better basis set than atomic orbitals for such metals. As pointed out by Ashcroft and Mermin, the tight-binding approximation "is most useful for describing the energy bands that arise from the partially filled d -shells of transition metal atoms and for describing the electronic structure of insulators."¹¹ Our results confirm this. A plane-wave basis set evidently has the required flexibility for the variational determination of valence s - p bands of proper stability for these metals. The atomic-orbital basis set also produces filled bands of about the proper width for these metals, but without sufficient stability. Bulk moduli for the s - p -band metals are calculated to relatively good accuracy with the ASED band method because they are functions of the second derivative of the total energy with respect to nuclear displacements. As has been shown elsewhere, force constants are a function of E_R in Eq. (4), provided that ρ_{npf} in Eq. (1) is well represented by fixed point charges during small displacements in nuclear positions.³⁵ This is still true for s - p -band metals, just as it is for the early transition metals, and the covalent and ionic solids examined here. It can be concluded that the atomic-orbital basis set simply lacks the flexibility of the plane-wave basis for putting enough bond charge where needed for the s - p -band metals.

For the covalent materials C, Si, and SiC the ASED band method, as described earlier,⁹ gives more accurate results than other semiempirical or empirical methods.³⁶⁻³⁸ The state of the art *ab initio* approaches³⁹⁻⁴¹ are even more accurate for most properties of these solids. However, the ASED band theory is relatively easy to apply to systems with large numbers of atoms in the primitive unit cell, such as needed to study interfacial bonding^{10,42} and polymers.⁴³

ACKNOWLEDGMENTS

We are thankful to M. H. Whangbo and W. R. L. Lambrecht for helpful consultation. The Defense Advanced Research Projects Agency (U.S. Department of Defense) supported their work through a grant, administered by the U.S. Office of Naval Research, to Case Western Reserve University.

¹A. B. Anderson, *J. Chem. Phys.* **62**, 1187 (1975).

²A. B. Anderson, R. W. Grimes, and S. Y. Hong, *J. Phys. Chem.* **91**, 4245 (1987).

³A. B. Anderson, *J. Chem. Phys.* **63**, 4430 (1975).

⁴R. W. Grimes, A. B. Anderson, and A. H. Heuer, *J. Phys. Chem. Solids* **48**, 45 (1987).

⁵A. B. Anderson, Ch. Ravimohan, and S. P. Mehandru, *Surf.*

Sci. **183**, 438 (1987).

⁶A. B. Anderson and Ch. Ravimohan, *Phys. Rev. B* **38**, 974 (1988).

⁷K. Nath and A. B. Anderson, *Phys. Rev. B* **39**, 1013 (1989).

⁸For a recent example, see S. P. Mehandru and A. B. Anderson, *Surf. Sci.* **201**, 345 (1988).

⁹K. Nath and A. B. Anderson, *Solid State Commun.* **66**, 277

- (1988).
- ¹⁰K. Nath and A. B. Anderson, *Phys. Rev. B* **38**, 8264 (1988).
- ¹¹See, for example, N. W. Ashcroft and N. D. Mermin, *Solid State Physics* (Saunders College, Philadelphia, 1976); T. A. Albright, J. K. Burdett, and M. K. Whangbo, *Orbital Interactions in Chemistry* (Wiley, New York, 1985).
- ¹²D. J. Chadi and M. L. Cohen, *Phys. Rev. B* **8**, 5747 (1973).
- ¹³S. L. Cunningham, *Phys. Rev. B* **10**, 4988 (1974).
- ¹⁴E. Clementi and D. L. Raimondi, *J. Chem. Phys.* **38**, 2686 (1963).
- ¹⁵J. W. Richardson, W. C. Nieuwpoort, R. R. Powell, and W. F. Edgell, *J. Chem. Phys.* **36**, 1057 (1962).
- ¹⁶W. Lotz, *J. Opt. Soc. Am.* **60**, 206 (1970).
- ¹⁷C. E. Moore, *Atomic Energy Levels*, Natl. Bur. Stand. (U.S.) Circ. No. 467 (U.S. GPO, Washington, D.C., 1958).
- ¹⁸E. Clementi and C. Roetti, *At. Data Nucl. Data Tables* **14**, 177 (1974).
- ¹⁹R. S. Tebble and D. J. Craik, *Magnetic Materials* (Wiley-Interscience, London, 1969), p. 63.
- ²⁰K. J. Chang and M. L. Cohen, *Phys. Rev. B* **30**, 4774 (1984).
- ²¹K. J. Chang, S. Froyen, and M. L. Cohen, *J. Phys. C* **16**, 3475 (1983).
- ²²P. K. Lam and M. L. Cohen, *Phys. Rev. B* **24**, 4224 (1981).
- ²³A. Bianconi, S. B. M. Hagström, and R. Z. Bachrach, *Phys. Rev. B* **16**, 5543 (1977).
- ²⁴G. Wiech and E. Zöpf, in *Electronic Density of States*, Natl. Bur. Stand. (U.S.) Spec. Publ. No. 323, edited by L. H. Bennett (U.S. GPO, Washington, D.C., 1971).
- ²⁵G. Wiech, in *Soft X-Ray Band Spectra*, edited by D. J. Fabian (Academic, London, 1968).
- ²⁶E. Kisker, K. Schröder, W. Gudat, and M. Campagna, *Phys. Rev. B* **31**, 329 (1985).
- ²⁷D. E. Eastman and J. L. Freeouf, *Phys. Rev. Lett.* **34**, 395 (1975).
- ²⁸D. Rieger, F. J. Himpsel, U. O. Karlsson, F. R. McFeely, J. F. Morar, and J. A. Yarmoff, *Phys. Rev. B* **34**, 7295 (1986).
- ²⁹S. Hufner, G. K. Wertheim, and J. H. Wernick, *Phys. Rev. B* **8**, 4511 (1973).
- ³⁰R. Y. Koyama and W. E. Spicer, in *Electronic Density of States*, Ref. 24.
- ³¹J. Callaway and C. S. Wang, *Phys. Rev. B* **16**, 2095 (1977).
- ³²R. A. Heaton and C. C. Lin, *Phys. Rev. B* **22**, 3629 (1980).
- ³³G. A. Burdick, *Phys. Rev.* **129**, 138 (1963).
- ³⁴Y. Wang, P. Nordlander, and N. H. Tolk, *J. Chem. Phys.* **89**, 4163 (1988).
- ³⁵A. B. Anderson, *Phys. Rev. B* **8**, 3824 (1973).
- ³⁶W. A. Harrison, *Phys. Rev. B* **27**, 3592 (1983).
- ³⁷O. F. Sankey and R. E. Allen, *Phys. Rev. B* **33**, 7164 (1986).
- ³⁸A. T. Paxton, A. P. Sutton, and C. M. M. Nex, *J. Phys. C* **20**, L263 (1987).
- ³⁹K. J. Chang and M. L. Cohen, *Phys. Rev. B* **35**, 8196 (1987).
- ⁴⁰M. T. Yin and M. L. Cohen, *Phys. Rev. B* **26**, 5668 (1982).
- ⁴¹W. R. L. Lambrecht and O. K. Anderson, *Phys. Rev. B* **34**, 2439 (1986).
- ⁴²K. Nath and A. B. Anderson, *Phys. Rev. B* **40**, 7916 (1989).
- ⁴³K. Nath and P. L. Taylor, *Mol. Cryst. Liq. Cryst.* (to be published).